

Ouachita Baptist University

## Scholarly Commons @ Ouachita

---

Honors Theses

Carl Goodson Honors Program

---

1995

### Dynamic Phase Steepening in Alfven Waves

Stephen R. Granade

*Ouachita Baptist University*

Follow this and additional works at: [https://scholarlycommons.obu.edu/honors\\_theses](https://scholarlycommons.obu.edu/honors_theses)



Part of the [Astrophysics and Astronomy Commons](#), [Elementary Particles and Fields and String Theory Commons](#), [Non-linear Dynamics Commons](#), and the [Plasma and Beam Physics Commons](#)

---

#### Recommended Citation

Granade, Stephen R., "Dynamic Phase Steepening in Alfven Waves" (1995). *Honors Theses*. 105.  
[https://scholarlycommons.obu.edu/honors\\_theses/105](https://scholarlycommons.obu.edu/honors_theses/105)

This Thesis is brought to you for free and open access by the Carl Goodson Honors Program at Scholarly Commons @ Ouachita. It has been accepted for inclusion in Honors Theses by an authorized administrator of Scholarly Commons @ Ouachita. For more information, please contact [mortensona@obu.edu](mailto:mortensona@obu.edu).

# SENIOR THESIS APPROVAL SHEET

This Honor's thesis entitled

**"Dynamic Phase Steepening in Alfvén Waves"**

written by

**Stephen R. Granade**

and submitted in partial fulfillment of the

requirements for completion of the

Carl Goodson Honors Program

meets the criteria for acceptance

and has been approved by the undersigned readers

Thesis Director

Second Reader

Third Reader

Director of the Carl Goodson Honors Program

April 15, 1995

Dynamic Phase Steepening in Alfvén Waves

by

Stephen Granade

Senior Honors Thesis

April 15, 1995

Our solar system contains more activity and complexity than can be seen through a telescope. One such "invisible" phenomenon is the solar wind, created by a steady stream of particles blasted away from the sun in all directions. The sun's donut-shaped magnetic field lines channel this stream. Particles moving along the field lines perform an intricate helical dance, with ions winding one way and electrons the other.

The solar wind shapes and is shaped by the magnetic fields of the planets and the sun. If left undisturbed by outside influences, the earth's magnetic field, like the sun's, would resemble a donut surrounding the earth (Fig. 1a). However, the solar wind constantly streams around the earth, and its pressure compresses the earth's magnetic field in front and elongates it in back, much like a comet's tail (Fig. 1b). This is known as a planetary bow shock.

Physicists have found that certain types of electromagnetic waves, called Alfvén waves, are formed in planetary bow shocks, near comets, and even within the solar wind itself (1). The waves, which are nonlinear, travel along the solar wind's magnetic field lines. If the field lines are represented by a stretched rubber band, Alfvén waves are represented by the wave that travels the length of the rubber band when it is plucked.

Since about 1968, scientists have sought a way to describe these waves mathematically (2). They have tried several equations, one family of which, the Derivative Nonlinear Schrödinger (DNLS) equation and its offshoots, has proven especially useful.

This paper will explain the origin of the DNLS equation in plasma physics, show its relationship to simpler wave equations, discuss the solution to the DNLS equation, and explain the numerical techniques used to find its eigenvalues. Eigenvalues are mathematical constructs which correspond to physically significant observables, such as a wave's velocity or amplitude. All of these topics will then be brought together to explain the new mechanism for phase steepening that was discovered in the course of the research by examining the DNLS equation's eigenvalues. The type of phase steepening explored by this research may serve to explain why only one of two different types of Alfvén waves have been observed in satellite data.

A plasma, as used here, is an electrically neutral, highly ionized gas composed of ions, electron, and neutral particles. It is effectively a state of matter that is distinct from solids, liquids, and normal gases. The solar wind, since it is comprised of ions and electrons, can be treated as a plasma. Waves in a plasma are well approximated by the formulas for magneto-hydrodynamic (MHD) waves. Ideal MHD waves depend on seven variables, and thus are described by seven independent equations. These equations have been developed in the study of fluid dynamics (3: 3.1), and roughly correspond to the conservation of mass, momentum, and energy for protons and electrons, with Maxwell's electromagnetic equations added to them. The ideal MHD equations are strongly nonlinear and do not take into account dispersive steepening of waves, which will be explained later. If dispersion is taken into account and some simplifications

made, the waves can be modeled using the Derivative Nonlinear Schrödinger (DNLS) equation. The DNLS equation has a weaker nonlinearity than the ideal MHD equations, yet is somewhat valid even for systems with strong nonlinearity.

The simplest types of waves are linear waves. In one dimension they can be described by the mathematical formula

$$u_t + cu_x = 0$$

which is the most general form of what is known as a harmonic wave. Its shape never changes; it moves forward with a constant speed of  $c$ .

The linear wave equation does not take into account dispersion, an effect found in all physical waves. Burger's equation adds a term for dispersion, which depends on the wave's second spatial derivative:

$$u_t + uu_x = \nu u_{xx}$$

The dispersion term  $\nu u_{xx}$  seems rather *ad hoc*, but it appears to model effects which are found in nature. Over time, friction and other forces cause any single wave to spread out, or disperse. The dispersion term mimics this effect by making the mathematical waves spread out. The nonlinear term  $uu_x$  leads to shocks within waves--higher amplitudes move faster, causing the waves to steepen (Fig. 2). The crest of the wave moves forward, forming a more vertical wave front.

Solitons form when nonlinearity and dispersion compete within a wave. Nonlinearity tends to steepen waves, while dispersion tends to spread waves out. Solitons are essentially

localized nonlinear wave packets. They have a unique property in that one soliton can interact with another, yet retain its individual characteristics. Soliton speed depends on amplitude: a "taller" soliton will overtake a "shorter." When the two solitons pass through each other, they each suffer only a mild phase shift; the waves are slightly ahead of where they were expected to be. No changes occur in their amplitude, scale-length, or speed (3: 9.1). The Korteweg-deVries (KdV) equation develops solitons over time:

$$u_t + uu_x = \delta u_{xxx}$$

The DNLS equation also forms solitons, as it balances steepening and finite ion inertia dispersion (3: 10.1) for weakly dispersive quasi-parallel Alfvén waves (5). The KdV equation has eigenvalues which are real numbers; however, the DNLS equation's eigenvalues are complex. The DNLS equation takes the form of

$$u_t + (|u|^2u)_x = iu_{xx}$$

The DNLS equation does not take into account finite electron inertia dispersion, only finite ion inertia dispersion.

Combining the DNLS equation with Burger's equation does take that dispersion into account. The DNLS-Burger's equation has the properties of both of its parent equations:

$$u_t + (|u|^2u)_x = i(1+i\delta)u_{xx}$$

Its eigenvalues are also complex. This research examined the evolution of the DNLS-Burger's equation's eigenvalues over time,

in order to find a possible mechanism for phase steepening.

All of the techniques described in this thesis, which were applied to the DNLS-Burger's equation for research purposes, also apply to the DNLS equation. Due to these considerations, the remainder of this thesis will discuss the DNLS equation.

The DNLS equation has been examined using the inverse scattering transform (IST). The DNLS equation and its offshoots are not directly integrable due to their nonlinearity. However, the IST allows the DNLS equation to be integrated indirectly by finding a linear scattering formula for the otherwise nonlinear DNLS equation. By integrating the DNLS equation, its eigenvalues may be found. Kaup and Newell (6) discovered the appropriate IST scattering problem for the DNLS equation:

$$\frac{\delta}{\delta x} \Phi(\lambda; x, t) = D(\lambda; x, t)\Phi$$

$$D = \begin{pmatrix} -i\lambda^2 & \lambda b(x, t) \\ \lambda b(x, t)^* & i\lambda^2 \end{pmatrix}$$

where  $\Phi$  is a 2 x 2 matrix. The solutions of the above matrix are known as the Jost functions,  $\Phi^\pm$ . The two Jost functions are linearly related by a scattering matrix  $S$ :

$$\Phi^-(\lambda; x, t) = \Phi^+(\lambda; x, t)S(\lambda; t)$$

where



$$S = \begin{pmatrix} S_{11} & S_{12} \\ S_{21} & S_{22} \end{pmatrix}$$

The eigenvalues of the DNLS equation occur where  $S_{11}(\lambda; t)$  is zero (5).

The function  $S_{11}(\lambda; t)$  is defined in the limit as  $x$  approaches infinity as

$$S_{11}(\lambda) = (\Psi_{1r} + i\Psi_{1i})(\cos[(u^2 - v^2)x_r] + i\sin[(u^2 - v^2)x_r])e^{-2uvx_r}$$

To integrate this function numerically, it must be divided into a real and an imaginary component:

$$S_{11r} = (\Psi_{1r}\cos[(u^2 - v^2)x_r] - \Psi_{1i}\sin[(u^2 - v^2)x_r])e^{-2uvx_r}$$

$$S_{11i} = (\Psi_{1i}\cos[(u^2 - v^2)x_r] + \Psi_{1r}\sin[(u^2 - v^2)x_r])e^{-2uvx_r}$$

As stated earlier, the eigenvalues of the DNLS occur where  $S_{11}(\lambda; t)$ , both the real and the imaginary parts, is zero.

Why use the IST? Because it is the simplest and most natural way of expressing the nonlinear character of the DNLS equation. The Fourier transform, a long-established technique for analyzing waves, is linear. Fourier analysis produces linear harmonics which are the most natural way to characterize a linear system. However, due to the nonlinear behavior of the DNLS equation, harmonics produced by Fourier analysis vary widely over time.

Instead, a complex nonlinear wave can usually be described

as the superposition of a few solitons. The solitons will not vary as widely over time as Fourier harmonics will. The IST is a soliton transform, and thus is well-suited for use with a nonlinear wave (1).

The DNLS equation has so-called "one-parameter" solitons, solitons in which there is a relationship between their amplitude and their speed. There are two types of one-parameter solitons: bright and dark. Bright solitons have an amplitude  $u$  greater than the background magnetic field strength  $u_0$ . Dark solitons have an amplitude  $u < u_0$  (2: 14).

The DNLS equation also has solitons which depend on two parameters and are thus called two-parameter solitons. They coil through space, and, when graphed, look much like a spring. The second parameter specifies in part how tightly wound the "spring" is. All one-parameter and two-parameter solitons correspond to an eigenvalue; finding the eigenvalues effectively finds the solitons. The behavior of the eigenvalues is mirrored by the behavior of the solitons.

We integrated the DNLS equation and examined the evolution of the its eigenvalues through time using computer-modeled numerical analysis. This numerical analysis utilized numerical approximations instead of pure mathematical solutions. Any numerical approximation tries to minimize numerical error. Over time, many techniques of minimizing errors have been developed. These techniques are more easily explained using simpler equations than the DNLS equation.

One of the simplest partial differential equations is

$$\frac{\delta u}{\delta t} = u_t = -c u_x = -c \frac{\delta u}{\delta x}$$

which is the equation for a harmonic wave. The easiest way of numerically approximating the above equation's evolution through time, a mathematical "brute-force" method, is by choosing a small  $\Delta t$  and  $\Delta x$  to replace the infinitesimally small  $\delta t$  and  $\delta x$  and by making an array of  $u$ 's:

$$u_j^{n+1} = u_j^n - \frac{\Delta t c}{2 \Delta x} (u_{j-1}^n - u_{j+1}^n) \quad (1)$$

The subscripts of  $u$  indicate changes over space; the superscripts of  $u$  indicate changes over time.

John von Neumann developed a method of determining whether a numerical approximation will become unstable, or "blow up," over time, now known as von Neumann analysis. He made the substitution

$$u_j^n = \xi^n e^{ikj \Delta x}$$

and then solved for  $\xi$ . A numerical method is unstable where the absolute value of  $\xi$  is greater than one.

Making the substitution into the approximation (1) and solving for  $\xi$  gives:

$$\xi = 1 - \frac{i c \Delta t}{\Delta x} \sin(k \Delta x)$$

No matter what value is chosen for the wavenumber  $k$ , the absolute value of  $\xi$  is greater than one. Specifically, at all

wavelengths, the equation increases exponentially; the approximation is numerically unstable.

The Lax method prevents some of this instability by averaging the spatial values of  $u$  used. It adds a term to damp the equation:

$$u_j^{n+1} = u_j^n - \frac{\Delta t c}{2 \Delta x} (u_{j-1}^n - u_{j+1}^n) + \frac{1}{2} (u_{j+1}^n - 2u_j^n + u_{j-1}^n)$$

If  $u_j$  becomes much larger than its neighbors  $u_{j-1}$  and  $u_{j+1}$ , then the damping term is negative, pulling the next value of  $u_j$  back down. Applying von Neumann analysis,  $\xi$  for this equation is

$$\xi = \cos k \Delta x - \frac{i c \Delta t}{\Delta x} \sin k \Delta x$$

$$\therefore |\xi| \leq 1 \quad \text{if} \quad \frac{c \Delta t}{\Delta x} < 1 \quad (\text{the Courant condition})$$

If the Courant condition is satisfied, then all wavelengths are damped, except as  $1/k$  approaches infinity. An increase in  $1/k$  corresponds to larger wavelengths, so that the practical effect is that long wavelengths are only weakly damped, while shorter, more unstable waves are more greatly damped.

The Lax method is effective because it introduces artificial smoothing, which tends to disperse waves. The averaging introduced by the Lax method has the same effect as dispersion.

This means that the Lax method cannot be used with Burger's equation, as the equation already has a dispersion term,  $\nu u_{xx}$ . This dispersion term would unsuccessfully compete with the

dispersion introduced by the Lax method. Nor can this method be used with the DNLS equation, since the Lax dispersion would override the DNLS equation's built-in dispersion.

Instead of trying to fix the brute-force method by adding or subtracting arbitrary terms, more sophisticated numerical techniques are employed. One such category of methods is the category of predictor-corrector methods. Predictor-corrector methods are based on the fact that any integral

$$y(x) = y_n + \int_x^{x_n} f(x', y) dx'$$

can be approximated by a polynomial

$$y_{n+1} = y_n + h'(\beta_0 y'_{n+1} + \beta_1 y'_n + \beta_2 y'_{n-1} + \dots)$$

where  $h'$  is the numerical stepsize  $\Delta x$  between successive  $y$ 's. If  $\beta_0$  is zero, the method is explicit; otherwise it is implicit. The first step of predictor-corrector methods is the predictor, or explicit, step, in which  $\beta_0$  is set to zero so as to find an initial value for  $y_{n+1}$ . That value of  $y_{n+1}$  is then used in the next step, the corrector step, in which  $\beta_0$  is nonzero. After each corrector step,  $y_{n+1}$  is closer to its actual value. Many corrector steps can be used; however, a point of diminishing returns is eventually reached (8: 740-741).

Finding the proper values for the  $\beta$  coefficients is a matter of trial and error involving no little amount of serendipity. To some extent it is magical; no one is sure why a given set of coefficients works while another does not. One of the more

successful predictor-corrector methods is the Adams-Bashforth-Moulton scheme. The third-order case, which was used in this research, is

$$y_{n+1} = y_n + \frac{h}{12}(23y_n - 16y_{n-1} + 5y_{n-2})$$

for the predictor step and

$$y_{n+1} = y_n + \frac{h}{12}(5y_{n-1} + 8y_n - y_{n-1})$$

for the corrector step.

Using the Adams-Bashforth-Moulton predictor-corrector method as part of a computer program, we integrated  $S_{11}(\lambda)$  and graphed the sign of its two parts at different  $\lambda$  on the complex plane, which is a Cartesian coordinate plane in which real values run along the x axis and imaginary values run along the y axis. In the computer program, four colors were assigned to the different signs of  $S_{11}$ : green if both the real and imaginary parts of  $S_{11}$  were positive, blue if the real part was positive and the imaginary part was negative, and so on. At each point on the complex plane,  $S_{11}$  was calculated and the proper color was plotted (Fig. 3a). The colors are grouped together, forming regions. Where the colors change, the sign of at least one of the two parts of  $S_{11}$  has changed; in other words, either part or all of  $S_{11}$  has passed through zero. Therefore, where four color regions intersect,  $S_{11}$  is zero, and an eigenvalue of the DNLS equation is located there (Fig. 3b). We are interested in the behavior of the eigenvalues; the values of  $S_{11}$  allow us to find

and record the eigenvalues and to see how they behave over time.

Previously, in Wyller and Mjølhus (9) and in Wyller *et al.* (10), the motion of a single complex eigenvalue in phase space was calculated from perturbation theory. It was found that the eigenvalue would, in general, travel in a counterclockwise circle which passes through the origin (Fig. 4). A numerical analysis of the eigenvalue showed that the results of the numerical solution and the idealized mathematical solution agreed well in regions III and IV, deviated slightly from each other in region II, and bore little resemblance to each other in region I. The numerical solution's deviations from the mathematical model indicate where non-soliton components of the wave develop, because the model assumes that any non-soliton component which develops is negligible and thus can be ignored (10).

However, what is the motion of eigenvalues which lie along the real axis? Take the case of a circularly polarized pulse:

$$u(x) = \begin{cases} b_0 & x > L \\ b_1 e^{i(kx + \phi_1)}, & |x| < L \\ b_0 e^{i\phi_0} & x < -L \end{cases}$$

We assumed that the pulse was traveling in a straight line, so that  $\phi_0$  would be zero. In addition, in order to make the equation continuous, the conditions  $b_0 = b_1$ ,  $\phi_1 = 0$ , and  $k \cdot L = 2\pi \cdot n$  had to be met. Hamilton, Kennel, and Mjølhus (11) showed that, in the weakly stable region ( $0 < k < b_1^2/2$ ), there will be two strings, or trains, of one-parameter solitons along the real axis, one bright and one dark. As the wavenumber  $k$  increases and



nears  $b_1^2/2$ , the leading eigenvalues of the two trains will be found closer and closer to each other. At the limit of the weakly stable region, the two solitons will coalesce, leaving only one two-parameter soliton in the complex plane (Fig. 5). This coalescence will continue in the weakly unstable region ( $b_1^2/2 < k < b_1^2$ ).

Increasing the wavenumber  $k$  makes the Alfvén wave, which resembles a spring when graphed, coil tighter and tighter. The distance between two successive "coils" of the wave decreases-- the "spring" is more tightly wound. This increase in  $k$  is known as phase steepening. According to Hamilton, Kennel, and Mjølhus, the increase in  $k$  is accompanied by the coalescence of the two one-parameter trains into one train of two-parameter solitons (11).

The computer program showed that this coalescence can occur dynamically as time progresses. Coalescence has been linked to phase steepening (11). Thus, phase steepening also occurs dynamically. This indicates that dissipation has the effect of modifying the wave's initial profile in such a way that the wavenumber  $k$  increases with time.

In addition, coalescence removes bright and dark soliton trains, converting the trains into two-parameter solitons. One-parameter solitons correspond to nonlinearly steepened waves, whereas two-parameter solitons correspond to phase steepened waves. When observational data has been taken of Alfvén waves, only phase steepened waves have been seen, not nonlinearly steepened waves (12). Coalescence may be able to explain why



only waves corresponding to two-parameter solitons are observed; the one-parameter solitons coalesce soon after the formation of Alfvén waves.

Now that dynamic phase steepening has been shown to occur, future research can try to establish a connection between phase steepening and an increase in the wavelength  $\lambda_1$ . If such a connection could be established, then the DNLS equation would reduce to the Nonlinear Schrödinger (NLS) equation, and Alfvén waves could be described by the NLS equation.

## References

1. T. Hada, R.L. Hamilton, and C.F. Kennel. The Soliton Transform and a Possible Application to Nonlinear Alfvén Waves in Space. *Geophys. Res. Lett.*, 20, 779, (1993).
2. T. Kakutani, H. Ono, T. Taniuti, and C.-C. Wei. Reductive perturbation method in nonlinear wave propagation II. Application to hydromagnetic waves in cold plasma. *J. Phys. Soc. Japan*, 24, 1159, (1968).
3. C.F. Kennel. Notebook, ms.
4. B.T. Tsurutani. Nonlinear Low Frequency (LF) Waves: Comets and Foreshock Phenomena. *Physics of Space Plasmas*, (1991).
5. R.L. Hamilton, C.F. Kennel and E. Mjølhus. Stability and Bifurcation of Quasiparallel Alfvén Solitons. *Phys. Scr.*, 46, 230, (1992).
6. D.J. Kaup and A. Newell. An Exact Solution for a Derivative Nonlinear Schrödinger Equation. *J. Math. Phys.*, 19, 798-801, (1978).
7. E. Mjølhus and T. Hada. Soliton Theory of Quasi-Parallel MHD Waves, ms.
8. Press, Teukolsky, Vetterling, Flannery. *Numerical Recipes in Fortran*. 2nd ed. Cambridge: Cambridge University Press, 1992.
9. J. Wyller and E. Mjølhus. A Perturbation Theory for Alfvén Solitons. *Physica D*, 13, 234, (1984).
10. J. Wyller, T. Flå and E. Mjølhus. The Effect of Resonant Particles on Alfvén Solitons. *Physica D*, 39, 405, (1989).

11. R.L. Hamilton, C.F. Kennel and E. Mjølhus. Formation of Quasiparallel Alfvén Solitons. *Phys. Scr.*, 46, 237, (1992).
12. B.T. Tsurutani and E.J. Smith, personal conversation, Sept. 23, 1994.

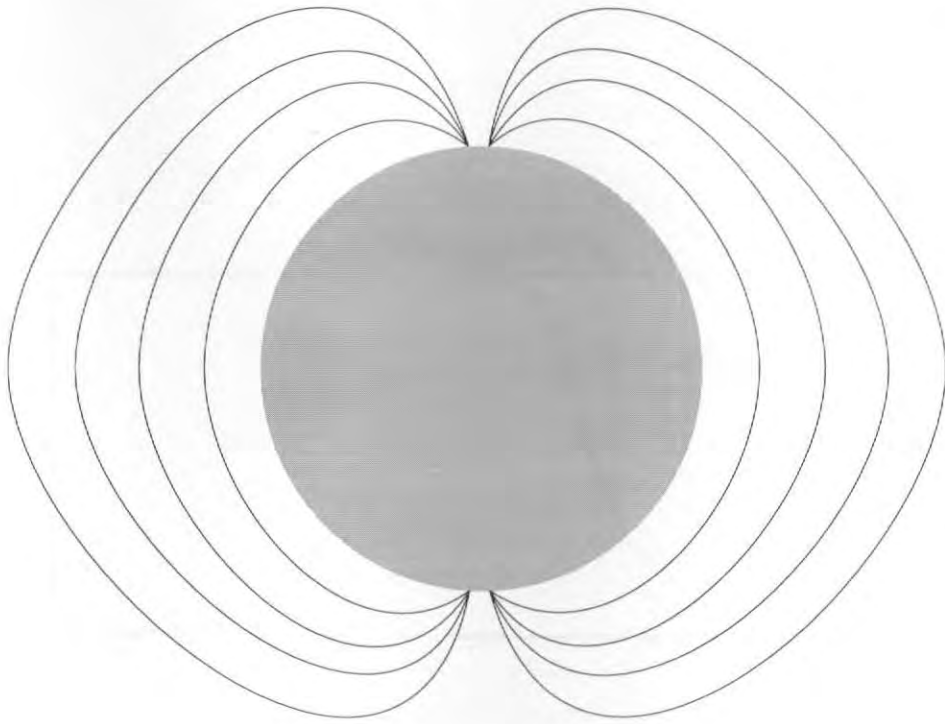


Fig. 1a: The earth's magnetic field if it were undisturbed

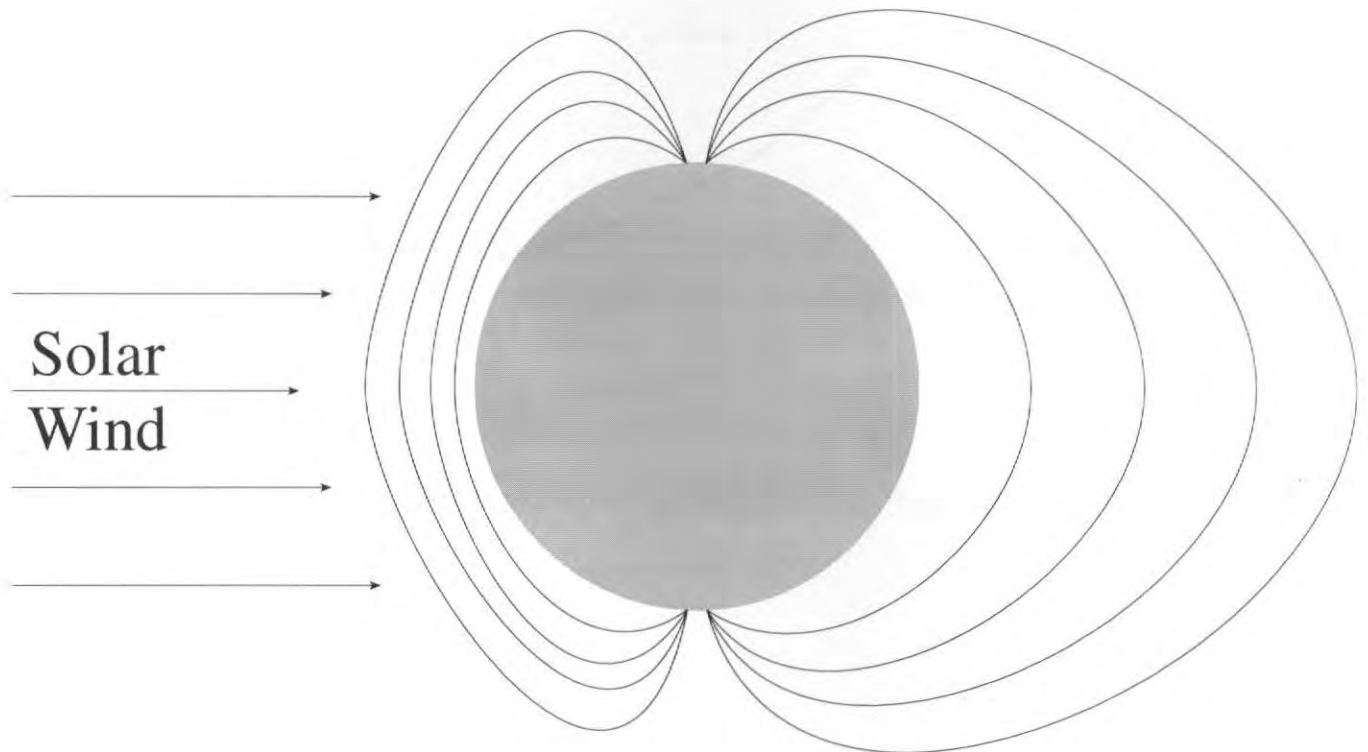
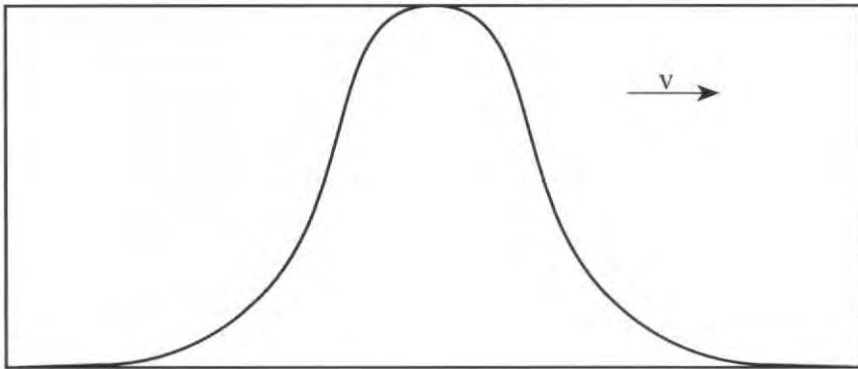


Fig. 1b: The earth's magnetic field as changed by the solar wind

Sinusoidal Wave



Steepened Wave

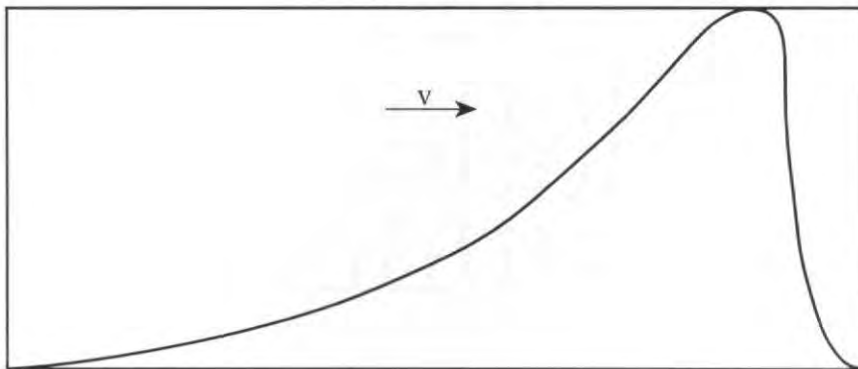


Fig. 2: Simplified example of wave steepening, adapted from Tsurutani [4]

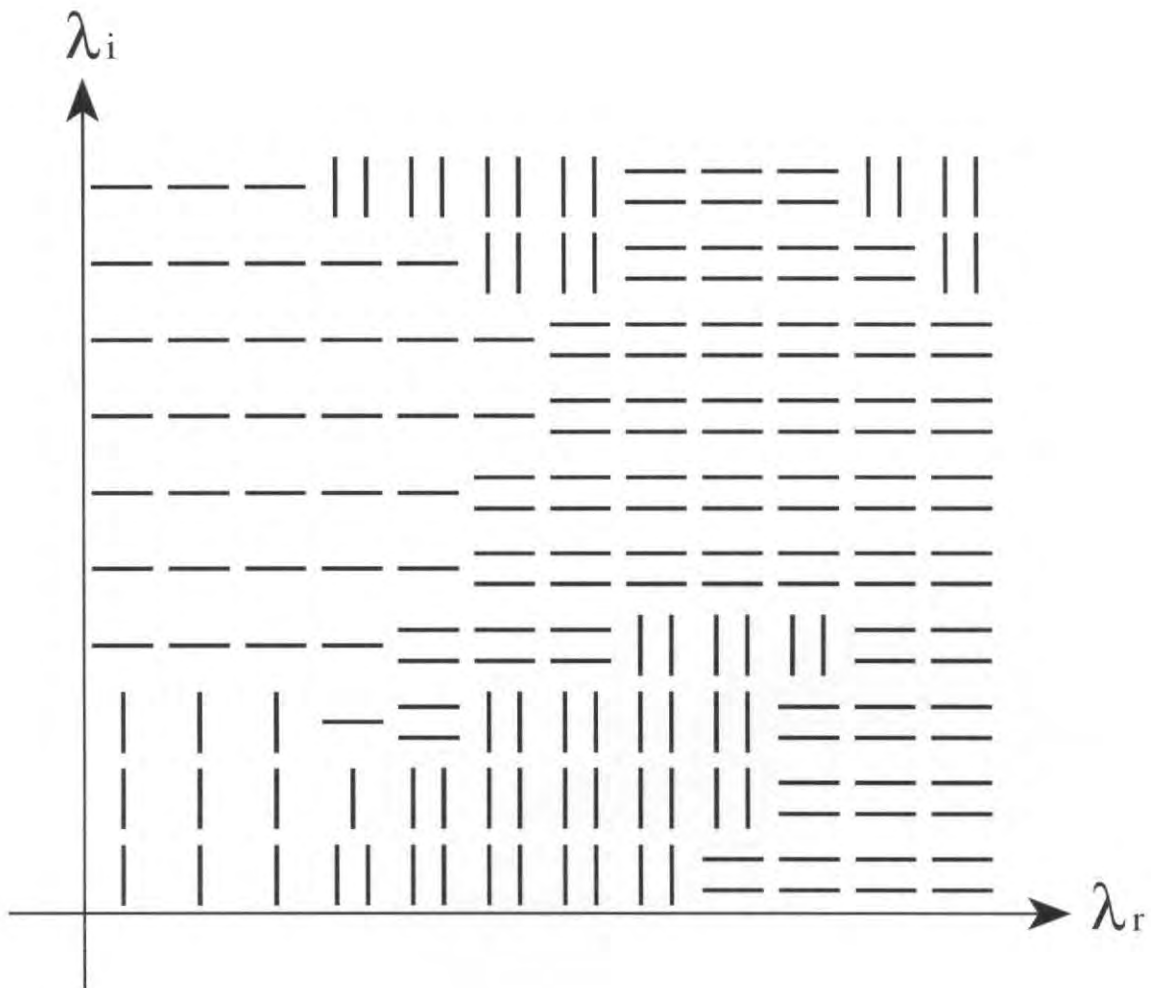


Fig. 3a: A graph of the values of  $S_{11}$ . The four different symbols represent the four different colors.



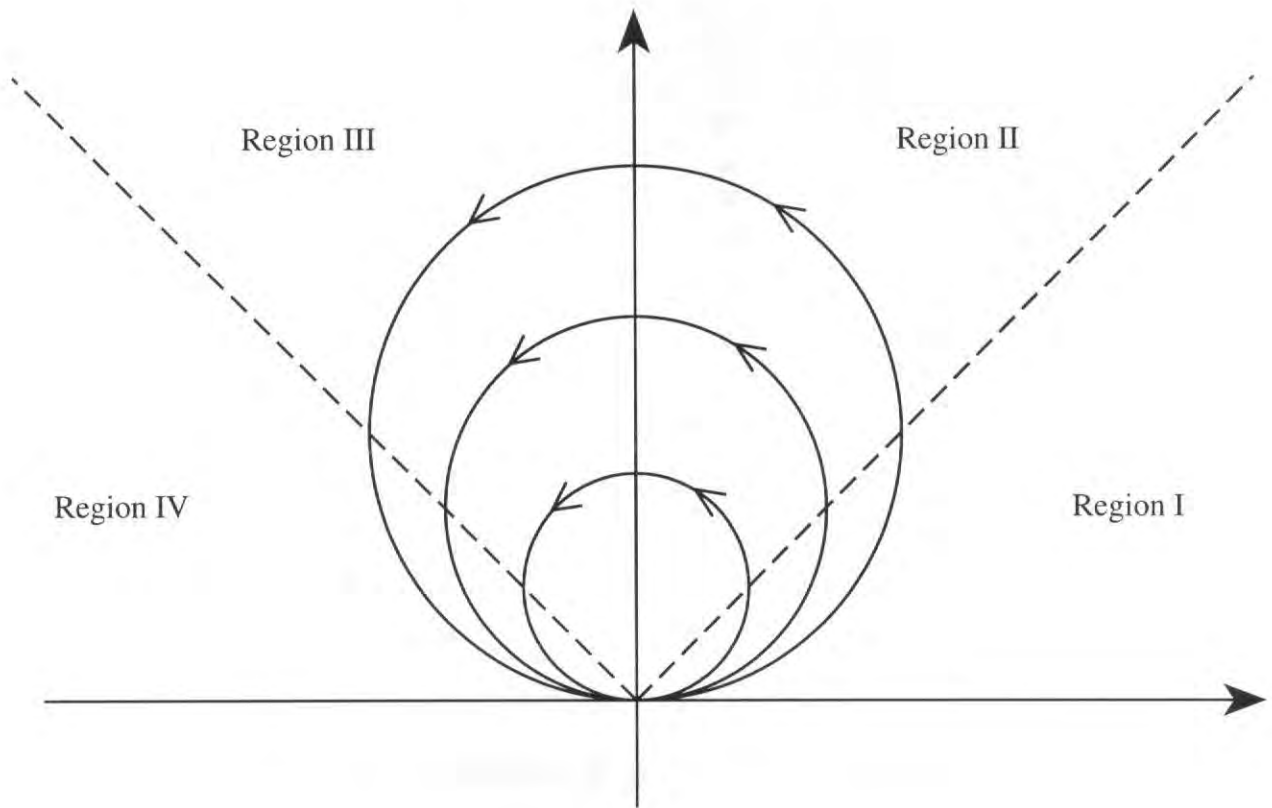


Fig. 4: The motion of a single eigenvalue, taken from J. Wyller et. al. [10]



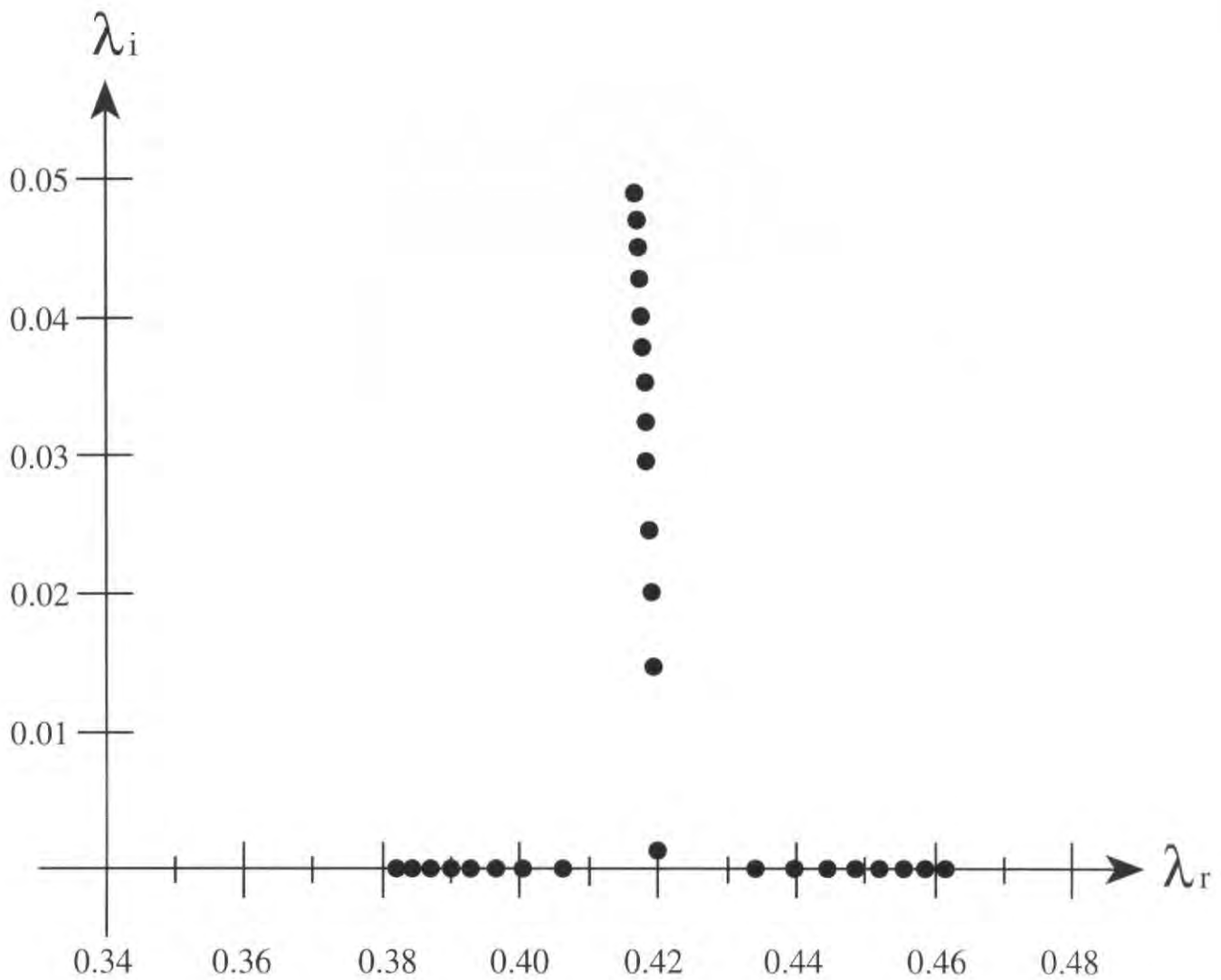


Fig. 5: The motion of two eigenvalues. The eigenvalues begin at about 0.381 and 0.462, then move towards each other. They coalesce at about 0.42, after which the remaining eigenvalue moves upwards. The values were taken at equal time intervals. Notice that the eigenvalues change slowly at first, speed up as they near coalescence, then slow down after coalescence.